

ICON and IFS model cloud evaluation using visible imagers on geostationary satellites

C. Stumpf, C. Köpken-Watts, L. Scheck*, R. Faulwetter, A. Seifert (DWD, *HERZ)
C. Lupu, T. Necker, S. Quesada-Ruiz, V. Firat, A. Benedetti (ECMWF)

Visible satellite channels provide valuable information on clouds, including their presence, location, and nature, complementing widely assimilated IR and MW data. Their integration enhances cloud and near-surface analyses and forecasts, particularly when combined with all-sky assimilation of corresponding IR channels. This capability has been demonstrated in DWD's regional NWP system, where SEVIRI 0.6 μm reflectances are operationally assimilated alongside the water vapor channels.

Recently, ECMWF assimilated visible data from the OLCI instrument into the global IFS system for the first time, assessing its impact on clouds and other key forecast variables (see poster by T. Necker, ECMWF).

To advance visible satellite data assimilation in the NWP systems of DWD and ECMWF, a joint evaluation of global ICON and IFS model cloud fields is conducted using geostationary imager data. This helps disentangle model and observation errors, provide feedback on model cloud physics, and improve the understanding of cloud-related biases.

1. Intercomparison setup

Visible reflectances from the geostationary imager ring (ABI on GOES-16/18, SEVIRI on Meteosat-9/10, and AHI on Himawari-9) provide a unique test bed that covers a wide range of atmospheric situations and different local times. Here we focus on the 0.6 μm channel and January 2024 period. To ensure optimal comparability between the ICON and IFS evaluations, we have taken steps to align the setups in both NWP systems as closely as possible:

Model resolutions:

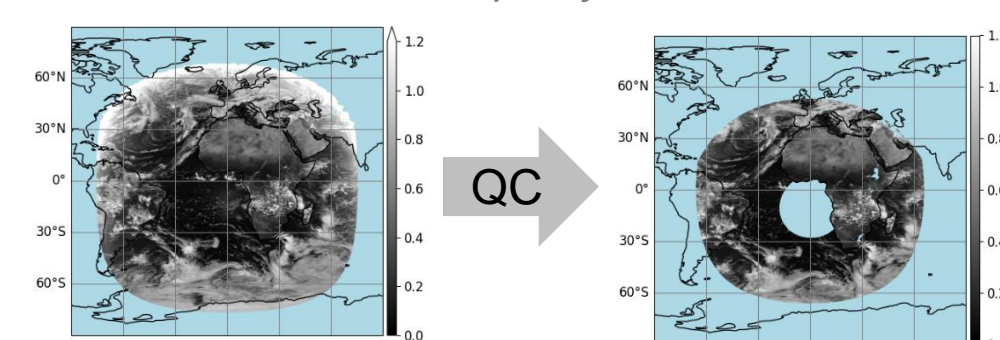
ICON at 26 km; IFS at 29 km.

Observation preprocessing:

ICON: Averaging onto grid cells, IFS: superobbing to approximately 29 km.

Quality control: Exclusion of data with large solar and satellite zenith angles, sun glint regions, sea ice and other surface and BRDF related aspects.

Satellite image of Meteosat-10 SEVIRI 0.6 μm channel before and after quality control



The model equivalents are derived from the ICON and IFS model fields using the fast neural-network-based MFASIS-NN solver in RTTOV-13.2, which is trained on simulated reflectances generated by the one-dimensional radiative transfer method DISORT (RTTOV-DOM). A key input for this process is the land BRDF atlas, specifically developed for this evaluation using January 2024 data from the MODIS Collection 6 (courtesy of J. Vidot, Meteotrance).

2. Assessment of ICON model physics modifications

Simulated versus observed SEVIRI 0.6 μm reflectances for different ICON physics setups

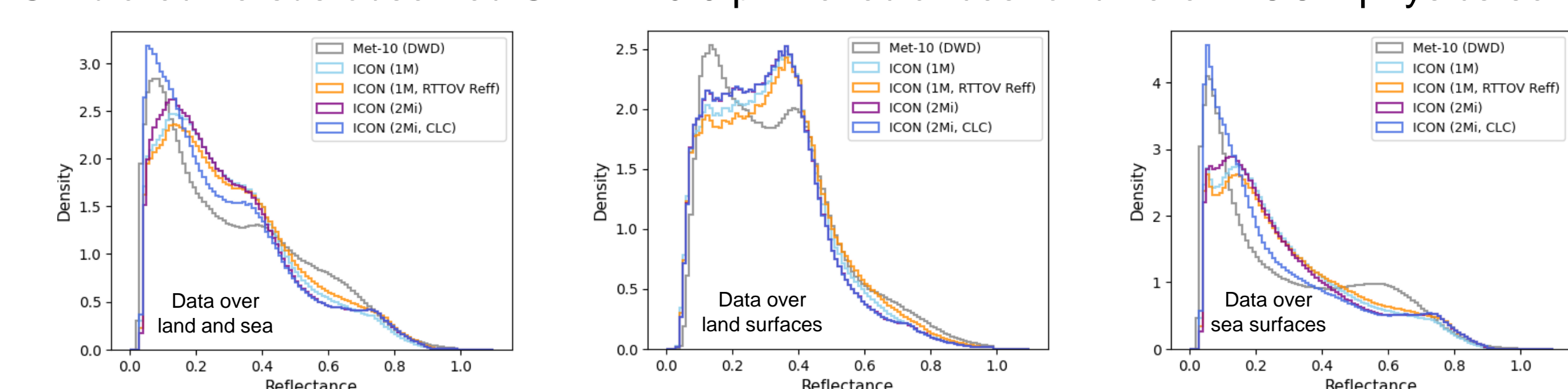


Fig. 1: SEVIRI (Meteosat-10) simulated reflectance histograms show the sensitivity to different radius parameterisations and ICON model cloud physics in comparison to observed 0.6 μm reflectances (Met-10): Results based on ICON model fields from the operational ICON one-moment scheme with ICON effective particle radii (1M) are compared to modified ICON versions where effective particle radii from Martin et al. (water clouds) and Wyser (ice clouds) provided by RTTOV (1M, RTTOV Reff), the improved ICON two-moment ice scheme with MODIS CDNCs (2Mi) or the ICON two-moment ice scheme with MODIS CDNCs and an additional ad hoc modification of the cloud cover scheme over ocean (2Mi, CLC) is used.

In addition to the intercomparison between ICON and IFS results, various ICON model physics modifications from the operational setup are evaluated and compared to observed reflectances. Fig. 1 shows the sensitivity of simulated reflectances using different assumptions for the effective cloud particles or modifications to the model cloud physics in comparison to the operational ICON model setup. Systematic differences to observed reflectances cannot be removed solely by the choice of effective particle radii or by

the improved representation of ice clouds in the two-moment ice scheme. The most significant impact arises from modifications to ocean cloud cover (final tuning pending), which lead to a substantially improved agreement between simulated and observed reflectances, especially for the peak at low reflectances associated with clear-sky conditions. This underscores the value of using visible reflectances to gain insights into model cloud physics and to drive model improvements.

3. ICON and IFS results in comparison to 0.6 μm reflectances

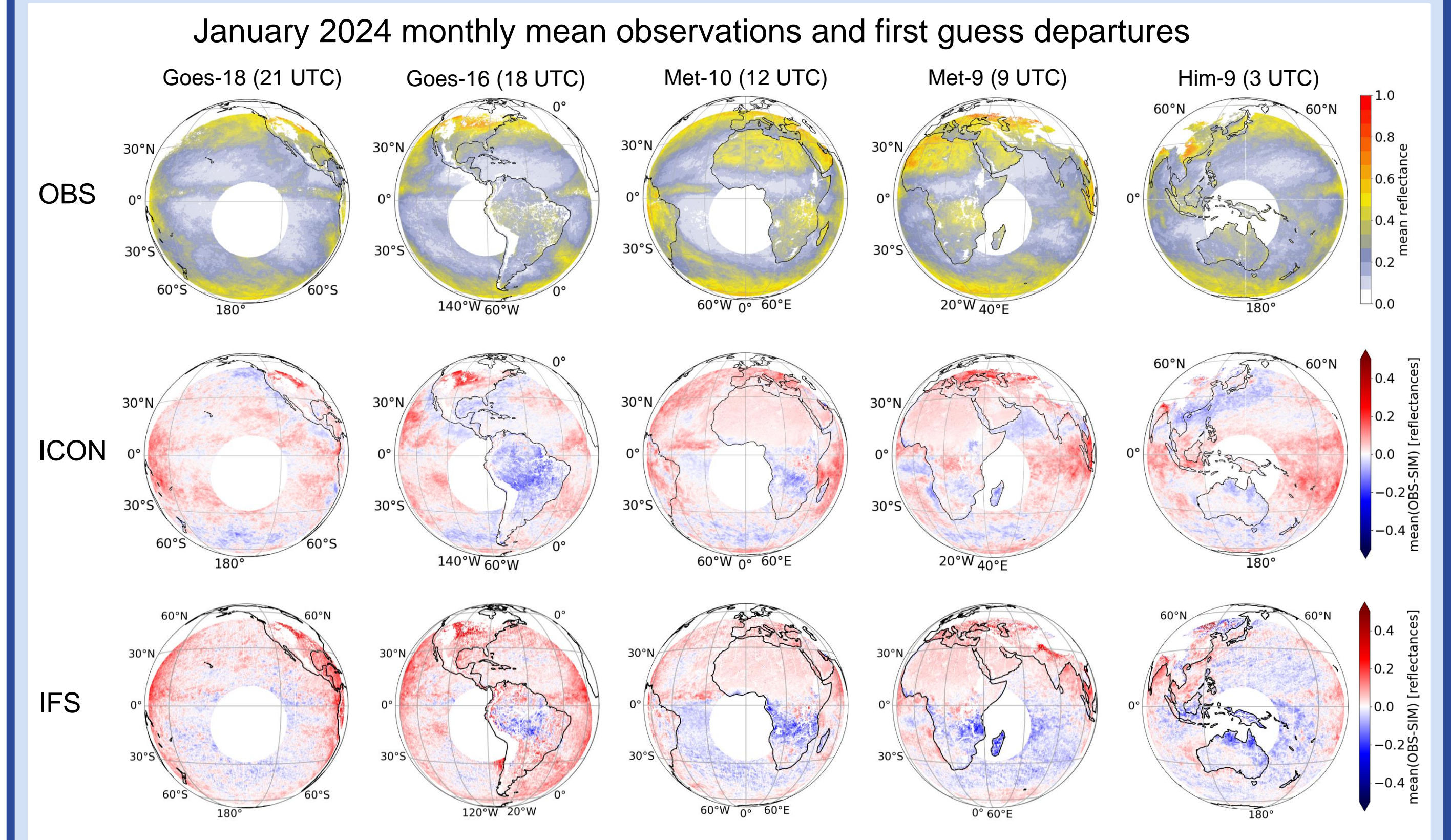


Fig. 2: Monthly means of observed 0.6 μm reflectances (top row) and monthly means of ICON (middle row) and IFS (bottom row) first guess departures for the five geostationary imagers. The ICON results shown are from the 2Mi, CLC setup, see Fig. 1.

Monthly mean first-guess departures on the map offer initial insights into typical regional model biases. Overall, the magnitude of differences is similar across all imagers and between the two NWP models. Larger biases are observed, for instance, over land in the northern regions, likely due to deficiencies in snow screening. This highlights the necessity for

further refinements in quality control processes. In the Amazonas region, where the ICON model is known to generate excessive cloud cover, ICON reflectances are noticeably higher compared to observations. For the IFS, peculiar biases appear for the Goes imagers, warranting closer examination.

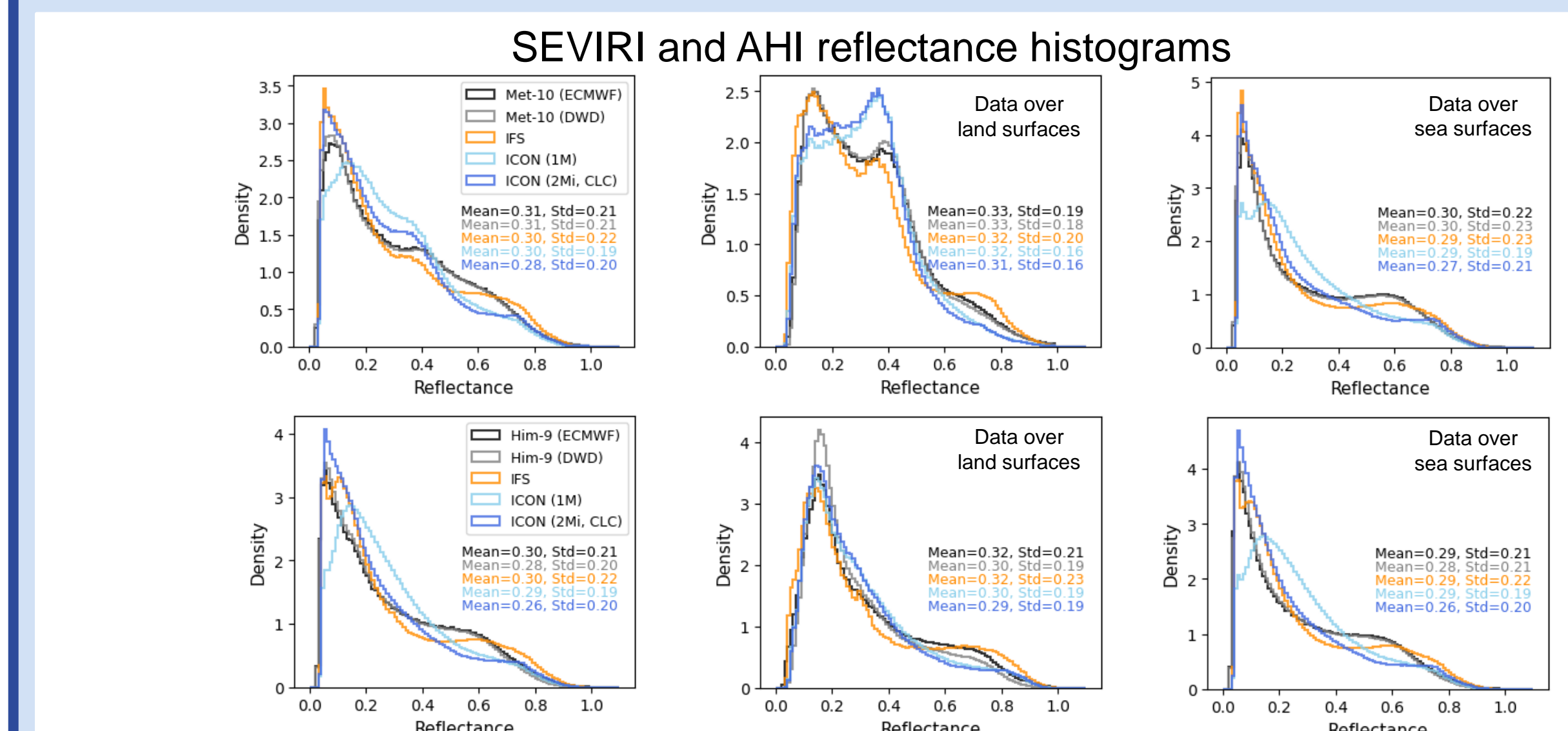


Fig. 3: Reflectance histograms for the 0.6 μm channel onboard SEVIRI (Meteosat-10, top row) and AHI (Himawari-9, bottom row) based on IFS and ICON model fields (operational 1M and improved 2Mi, CLC model physics setup) compared to observations as preprocessed at ECMWF (in black) and DWD (in grey).

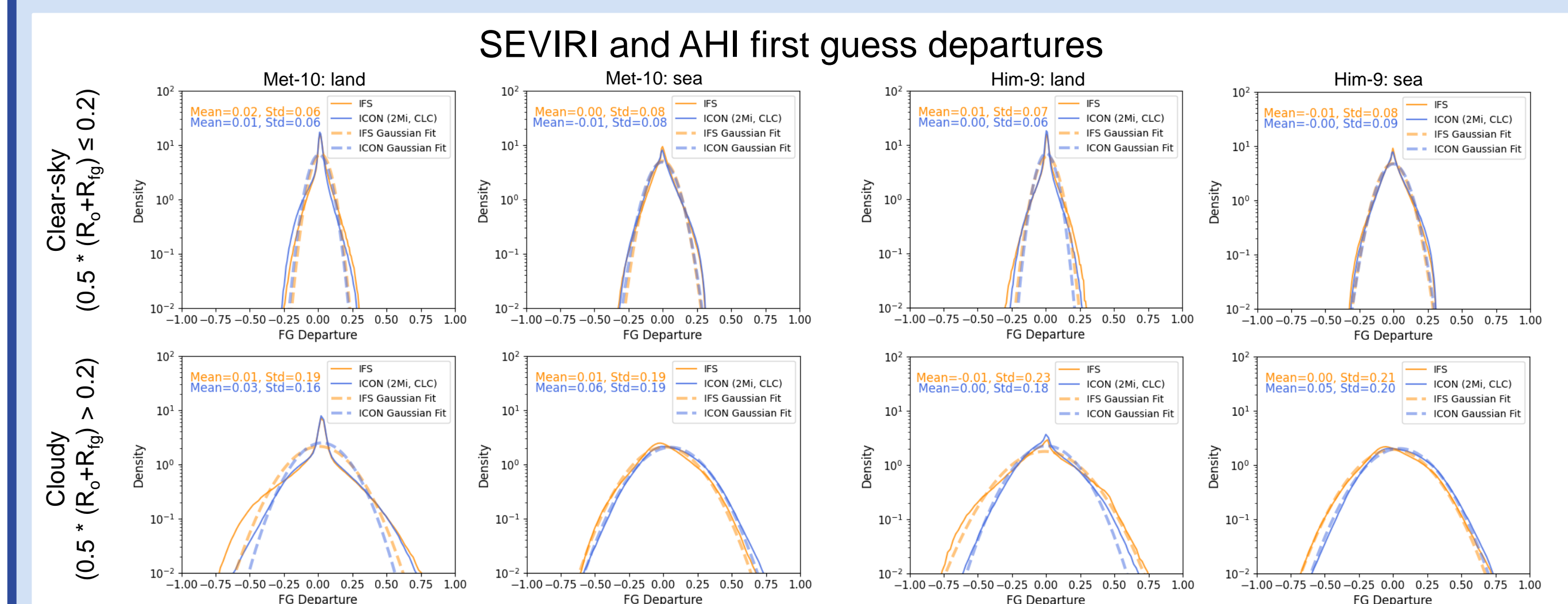


Fig. 4: First guess departures based on IFS and ICON model fields (improved 2Mi, CLC model physics setup) and 0.6 μm channel reflectances from SEVIRI (Meteosat-10, left) and AHI (Himawari-9, right) stratified according to surface type and clear-sky and cloudy situations.

The study of reflectance histograms (Fig. 3) and first guess departures (Fig. 4), stratified by surface type and atmospheric condition (clear-sky/cloudy), represents a first step toward a situation-dependent analysis of observation errors and biases. The overall shape of the reflectance histograms is well captured, and the first guess departures are relatively symmetric and unbiased. However, departures under cloudy conditions exhibit significantly larger

standard deviations indicating the need for a cloud-dependent error model. Further regional and situation-dependent analyses are crucial for a deeper understanding of the differences between simulated and observed reflectances, as well as for defining observation error models, refining quality control approaches, and addressing a potential need for bias corrections.

